

## OPTICAL PROPERTIES OF InGeSe THIN FILMS

M M Abd El-Raheem, H. A. Abd Alghany, M. M Wakkad , A. M. Abousehly<sup>a</sup>,  
N. A. Abd-Allah<sup>\*</sup>

*Department of physics, Sohag University, Faculty of science, Sohag, Egypt*  
*Al-Azhar University, Faculty of Science, Assuit, Egypt*

Effect of composition and annealing temperature on the optical properties of  $\text{In}_8\text{Ge}_x\text{Se}_{92-x}$  ( $14 \leq x \leq 25.5$ ) thin films deposited by electron beam from bulk samples prepared using melt quench technique are investigated and discussed. All films have amorphous structure. It was found that the electronic energy gap  $E_g$  increases with increasing Ge contents and has an abrupt change at coordination number  $Z \geq 2.65$ . The ratio of free carrier concentration to the carrier effective mass ( $N/m^*$ ) and the high frequency dielectric constant  $\epsilon_\infty$  showed also abrupt change at  $Z \geq 2.65$ . The optical relaxation time  $\tau$  found to have a minimum value at  $Z = 2.65$ . The optical energy gap  $E_g$  found to be affected by annealing.

(Received January 15, 2009; accepted January 21, 2009)

*Keyword:* InGeSe, Optical gap, Refractive index, Relaxation time, Dispersion energy

### 1. Introduction

Chalcogenide glasses are very interesting materials for technical applications in many fields such as electronics, optoelectronics, memory image storage and infrared optics, this is because of their physical properties are strongly dependent on their composition [1-2]. They exhibit distinguished phenomena, which are applicable for devices such as electrical switching and/or memory storage and photoresistors [3-4]. Optical fibers used in the mid infrared optical region, peculiarly from 2 to 12  $\mu\text{m}$  are the basis of many applications [5-6]. The optical properties of amorphous semiconductors are known to be sensitive to the preparation conditions [7]. Also, various optical properties of chalcogenide glasses have been reported [8-9]. On the other hand, a lot of work has been done on bulk and thin film glassy germanium chalcogenide regarding the electrical, optical properties and crystallization kinetics [10-13]. Other studies have been done also on alloys of different compositions of selenium and tellurium regarding the amorphous-crystalline transition [14-17].

It is generally recognized that most of the chalcogenide glasses show p-type conduction and their electrical conductivity is very slightly affected by doping, which is attributed to the presence of charged defects, which pin the Fermi level near the midgap [18].

Structural studies of chalcogenide materials using various techniques are very important for better understanding of their transport mechanisms and thermal stability. On the other hand, studies on the crystallization of a glass upon heating can be performed in several ways. In calorimetric measurements, two basic methods can be used, isothermal and non-isothermal. However, the results of crystallization process can be interpreted in terms of several theoretical models [19-20].

The aim of the present work is study the optical parameters as a function of the Ge content, coordination number and annealing time.

## 2. Experimental technique

Elemental constituents of high purity (5N) were used for preparing bulk glasses of the composition  $\text{In}_8\text{Ge}_x\text{Se}_{92-x}$  ( $14 \leq x \leq 25.5$ ) using the conventional melt quenching technique.

The films of the present compositions were prepared on ultrasonically cleaned corning glass using the electron beam evaporation in a coating system (Edward's High vacuum coating unit model 306A, U.K.) under a pressure of  $5 \times 10^{-6}$  Torr. The thickness of the film was controlled to be in the 100-200nm range by means of a film thickness monitor (Edward's High vacuum FTM5 thickness monitor, U.K.). The deposition rate was about 2nm/s.

Optical transmission and reflection were measured over the wavelength range 200 – 2500 nm using a Jasco V – 570 – visible – NIR spectrophotometer with a scan speed of 1000 nm/min.

The amorphous nature of the studied compositions either as-prepared or annealed bulk and/or films forms were confirmed by X-ray diffraction (XRD) pattern using X-ray diffractometer type philps (Holland) model PW1710.

A calibrated differential scanning calorimeter (DSC) type Shimadzu (Japan) model DSC-50 is used for studying the thermal behaviour of the considered compositions.

## 3. Results and discussion

### 3.1 Effect of composition

Fig.(1) shows the spectral variation of  $\text{In}_8\text{Ge}_x\text{Se}_{92-x}$  amorphous thin films in the spectral 0.2 – 2.5  $\mu\text{m}$  range. The absorption edge of the investigated compositions is in the range of visible spectral range, where its transmission fall to about zero values at  $\lambda \approx 0.3 \mu\text{m}$ . Hence, it can be revealed that the electronic energy gaps of the considered thin films are in the range of the energy of visible region.

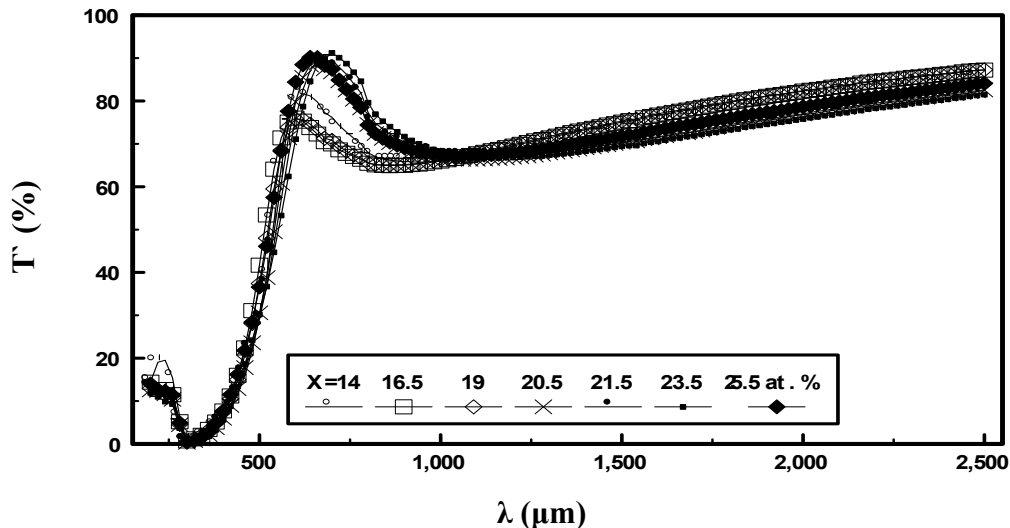


Fig. 1. Spectral dependence of the transmittance ( $T$ ) for as-deposited  $\text{In}_8\text{Ge}_x\text{Se}_{92-x}$  thin films.

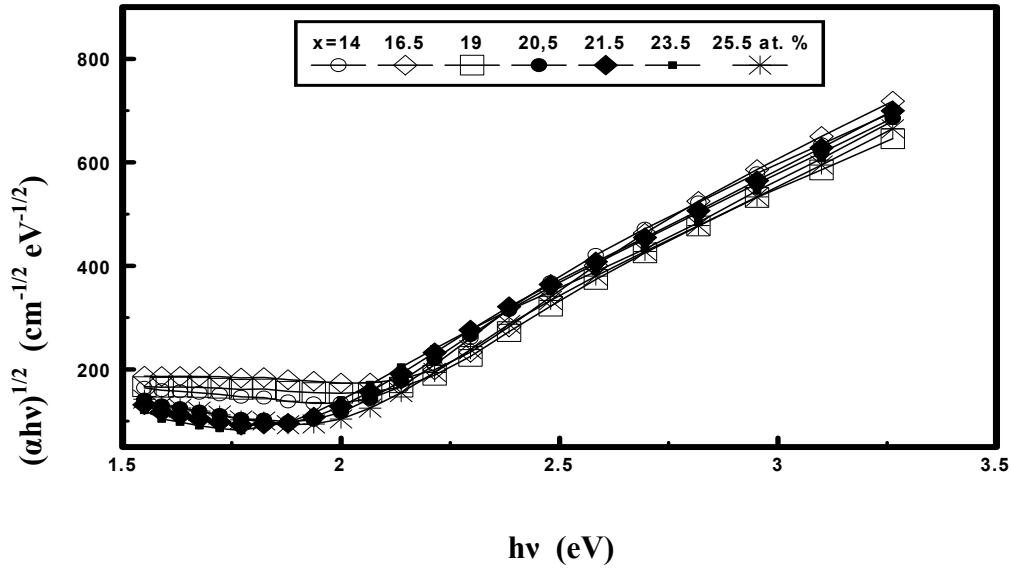


Fig. 2. Plots of  $(\alpha hv)^{1/2}$  vs.  $hv$  for as-deposited  $In_8Ge_xSe_{92-x}$  ( $14 \leq x \leq 29.5$  at. %) thin film.

The absorption coefficient  $\alpha$  of the investigated amorphous thin films can be calculated using Tauc equation [21] as follows;

$$\alpha(\nu) = \beta (h\nu - E_g)^2 / h\nu \quad (1)$$

where  $E_g$  is the electronic energy gap and  $\beta$  is an energy independent constant.

The plots of  $(\alpha hv)^{1/2}$  versus  $hv$  for a set of  $In_8Ge_xSe_{92-x}$  amorphous thin films of thickness equal to 100nm as an example are shown in Fig.(2) where both  $E_g$  and  $\beta$  values can be obtained. The calculated  $E_g$  values found to increase with Ge contents as recorded in table 1. This behavior can be accepted because, the calculated binding energy  $\langle E \rangle$  of the investigated compositions increases with increasing of Ge content as mentioned in table (1)

Table 1. Variations of the density  $d$  ( $gm\ cm^{-3}$ ), the average coordination number  $Z$ , the parameter  $r$  represents the deviation from stoichiometry, the overall mean bond energy  $\langle E \rangle$  (eV), the optical gap  $E_g$  and the glass transition temperature  $T_g(K)$  at  $Q = 10\ K\ min^{-1}$  with germanium ratio, for  $In_8Ge_xSe_{92-x}$

X(at.%)	$d(gm.cm^{-3})$	$Z$	$r$	$\langle E \rangle$ (eV)	$E_g$ (eV)	$T_g(K)$ at $Q = 10\ K\ min^{-1}$
14	3.9522	2.52	1.682	2.429	1.590	479.04
16.5	4.0014	2.57	1.459	2.519	1.600	458.79
19	4.1282	2.62	1.278	2.614	1.630	485.72
20.5	4.2088	2.65	1.184	2.672	1.640	523.25
21.5	4.4366	2.67	1.127	2.712	1.720	539.33
23.5	4.4949	2.71	1.024	2.794	1.730	569.85
25.5	4.5750	2.75	0.933	2.936	1.733	592.00

In fact the valence and conduction bands in chalcogenide glasses are constituted by lone-pair and antibonding bands. Thus the increase of the average bond energy of the system leads to

the increase of the energy of the conduction band edge and thereby  $E_g$  increases. As it is known, the variation of the physical properties of chalcogenide glasses against their chemical compositions can be discussed on terms of the chemically ordered network model and the topological model. The peculiarity of the compositional dependence of  $E_g$  observed at Ge content = 20.5 at.% could not be discussed in terms of the chemical ordered network model because the considered compositions are nonstoichiometric as it is revealed by the parameter  $r$  in table(1). Table 1 reveals also that there is an abrupt change in  $E_g$  at  $Z = 2.65$  which may confirm the validity of the topological model based on the structural consideration to explain the present compositional dependence of  $E_g$ . Furthermore, the results show that  $E_g$  increases with increasing film thickness. This can be interpreted as, the unsaturated bonds are produced as a result of an insufficient number of atoms deposited in the amorphous films [22]. These unsaturated bonds are responsible for the formation of some defects in the film, which produce localized states in its band gap. Whereas, in the case of thicker films, great deposition builds up more homogeneous network which minimizes the number of defects and the localized states thereby increasing the electronic energy gap.

Fig.(3) shows the spectral dependence of the films reflectivity ( $R'$ ) for the investigated  $In_8Ge_xSe_{92-x}$  ( $14 \leq x \leq 25.5$  at.%) system.

Assuming that the frequency of the optical spectrum is relatively high since the present reflectivity measurements were performed up to the near infrared spectrum region, the real ( $\epsilon'$ ) and imaginary ( $\epsilon''$ ) parts of the complex dielectric constant can be written by the following relations;

$$\epsilon' = n_o^2 - k'^2 = \epsilon_\infty - (e^2 N \lambda^2) / (4 \mu^2 c^2 \epsilon_o m^*) \quad (2)$$

$$\epsilon'' = 2 n_o k' = [( \epsilon_\infty \omega_p^2 ) / ( 8 \pi c^3 \tau )] \lambda^3 \quad (3)$$

where

$$\omega_p = ( e^2 N / \epsilon_o \epsilon_\infty m^* )^{1/2} \quad (4)$$

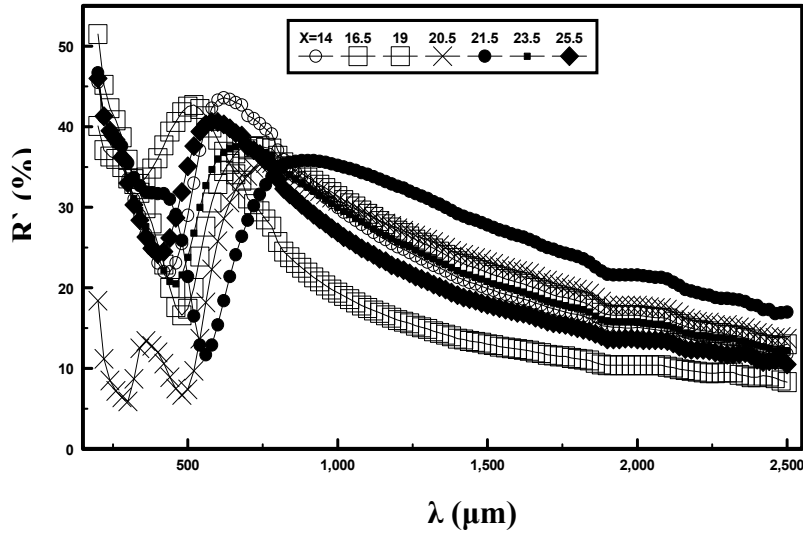


Fig. 3. Spectral dependence of the reflectivity ( $R'$ ) for as-deposited  $In_8Ge_xSe_{92-x}$  thin films.

is the plasma resonance frequency for one kind of free carriers,  $\epsilon_\infty$  is the high frequency dielectric constant,  $e$  is the electronic charge,  $c$  is the velocity of light,  $\epsilon_o$  is the free space dielectric constant,  $N/m^*$  is the ratio of free carrier concentration  $N$  to the free carrier effective mass  $m^*$  and

$\tau$  is the optical relaxation time. The last equations were used to determine the parameters  $\epsilon_\infty$ ,  $N/m^*$ ,  $\omega_p$  and  $\tau$ .

Figs.(4-5) show the variations of both  $\epsilon'$  and  $\epsilon''$  with  $\lambda^2$  and  $\lambda^3$  of the as-deposited  $\text{In}_8\text{Ge}_x\text{Se}_{92-x}$  respectively. The present data in the mentioned two figures are linear which confirm eqs.(2&3) leading to the possibility of calculating  $\epsilon_\infty$ ,  $N/m^*$ ,  $\omega_p$  and  $\tau$  of the investigated thin films.

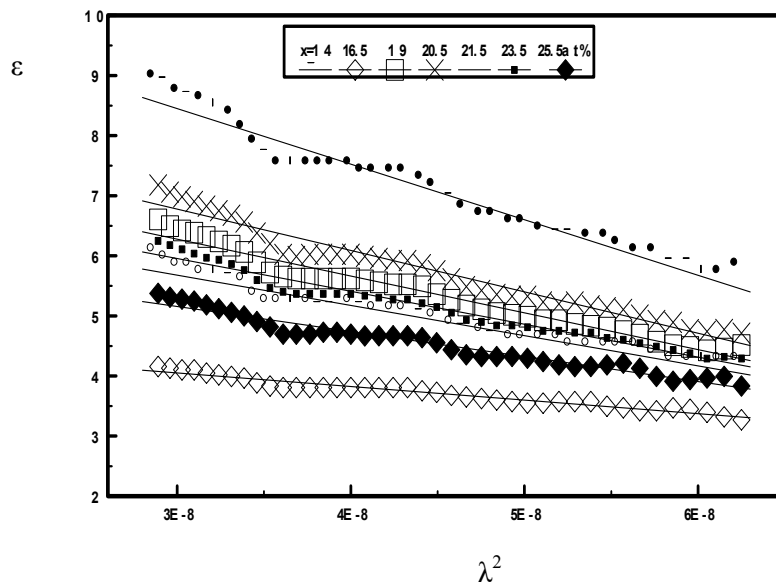


Fig. 4. Variations of the real part of  $\epsilon'$  with  $\lambda^2$  for as-deposited films.

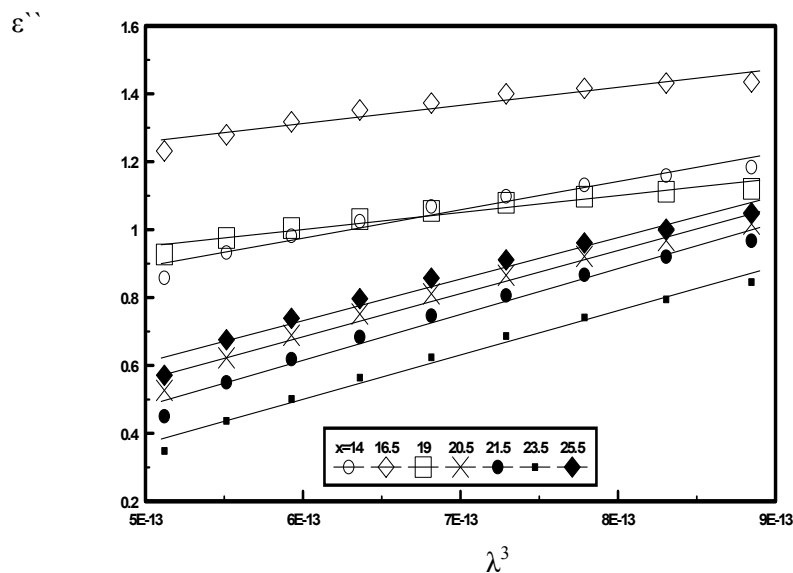


Fig. 5. Variations of  $\epsilon''$  with  $\lambda^3$  for as-deposited films.

Fig.(6) shows the variation of both  $N/m^*$  and  $\epsilon_\infty$  with  $Z$ . It is obvious that there is an abrupt change at  $Z = 2.62$  which can be correlated to the peculiarity observed at  $Z = 2.67$  for network chalcogenide glasses, which was attributed to a change from two-dimensional (2D) layered structure to three dimensional (3D) network arrangement due to cross-linking. Besides, this unusual similarity in  $\epsilon_\infty$  and  $N/m^*$  behaviour has been observed for p-type  $\text{P}_b - \text{S}_n - \text{Te}$  chalcogenide system, which has been attributed to the relatively higher carrier concentration

which is consistent with the present case (Assuming that  $m^*$  is a constant in the first approximation with the present case).

The values of the plasma edge deduced for the present amorphous chalcogenide lie in the higher  $2.22 \leq \lambda_p(\mu\text{m}) \leq 2.30$  frequency range, are inconsistent with the results reported for semiconductors [23], where the plasma edge lie in  $10 - 100 \mu\text{m}$  of infrared region. On the other hand, the plasma edge could be observed in the ultraviolet spectral range in case of metals due to their relatively higher free carrier concentration [23]. Thus the shift of plasma edge towards high frequency in the present case could be attributed to the relatively higher values of carrier concentration as mentioned before.

Fig.(7) shows the variation of the optical relaxation time  $\tau$  with the average coordination number  $Z$ , clearly, the obtained  $\tau$  values which have a minimum at  $Z = 2.65$  may be related to the abrupt change of both  $\epsilon_\infty$  and  $N/m^*$  occurred at the same value of  $Z$ . This correlation can be predicted from the relation;

$$\tau = 2\pi / \omega_p = 2\pi(e^2N / \epsilon_0 \epsilon_\infty m^*)^{-1/2} \quad (4a)$$

Moreover, the obtained values of  $\tau$  for the present compositions, which are in the  $0.01 \times 10^{-14} - 0.035 \times 10^{-14}$  s range are relatively small compared with those reported for some chalcogenides [24] by amount of one order of magnitude. These small values of  $\tau$  can be attributed to the higher concentration of free carriers possessed in the present materials. The refractive index  $n$  at photon energy  $E$  can be expressed as;

$$n^2 - 1 = (E_d E_0) / (E^2 - E_d) \quad (5)$$

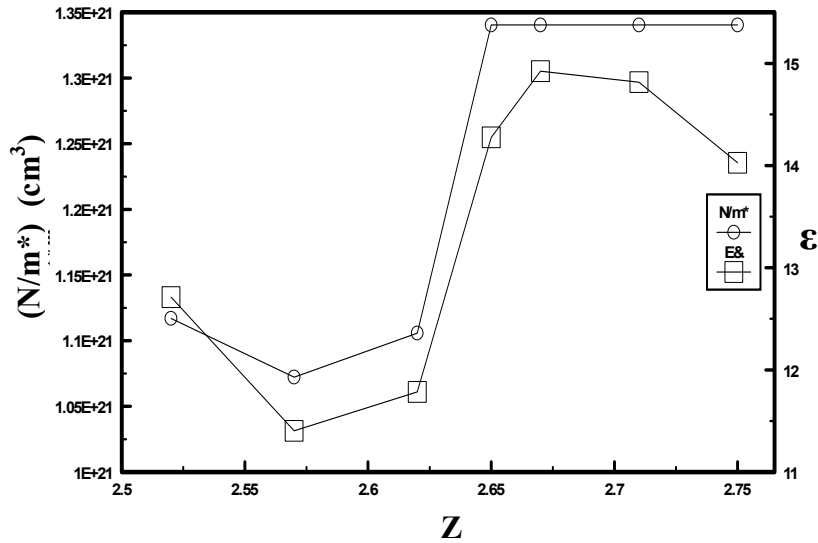


Fig. 6. Variations of both  $(N/m^*)$  and  $\epsilon_\infty$  with the average coordination number  $Z$  for as-deposited  $\text{In}_8\text{Ge}_x\text{Se}_{92-x}$  thin films.

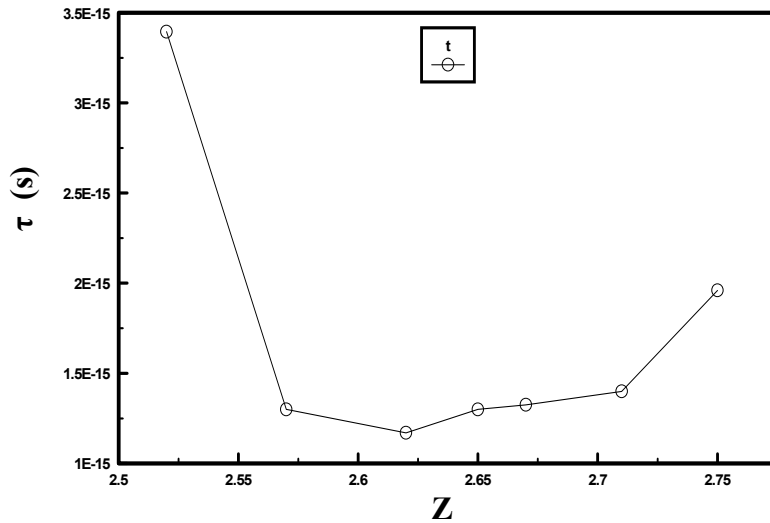


Fig. 7. Variation of  $\tau$  with the average coordination number  $Z$  for as-deposited  $In_8Ge_xSe_{92-x}$  thin films.

Where  $E_d$  is the electronic dispersion energy,  $E_o$  is the single oscillator energy. The values of  $E_d$ ,  $E_o$  and  $n$  can be obtained from the slope and intercept of the  $[n^2 - 1]^{-1}$  versus  $E^2$  plot. Fig.(8) depicts the spectral variation of the refractive index  $n$  of the  $In_8Ge_xSe_{92-x}$  amorphous thin films in near infrared optical region. The general features of this figure are as follows: I- The observed  $n - \lambda$  behaviour is as the usual one, where generally the values of  $n$  decreased with the increase of  $\lambda$  towards the plasma edge.

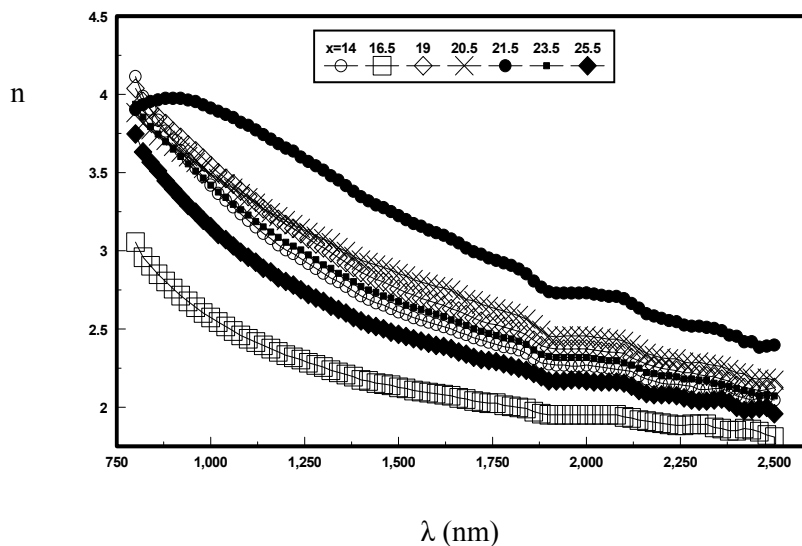


Fig. 8. Variations of refractive index ( $n$ ) with wavelength ( $\lambda$ , nm) for  $In_8Ge_xSe_{92-x}$  thin films.

II- The absolute values of  $n$  in low wavelength range of near infrared spectra are relatively high. This may be attributed to the high free carrier concentration in the present materials.

Fig.(9) shows the  $[(n^2 - 1)^{-1}]$  versus  $(h\nu)^2$  variation. The observed dependence have a linear shape which confirm the equation (5).

The variation of the calculated values of  $E_d$  and  $E_o$  with  $Z$  reveal that all of them have a maximum at  $Z = 2.67$  which can be attributed to the structural rearrangement (topological phase transition from 2D to 3D). Also, it can be seen that, values of  $E_d \approx 10E_g$  and  $E_o \approx 2E_g$ .

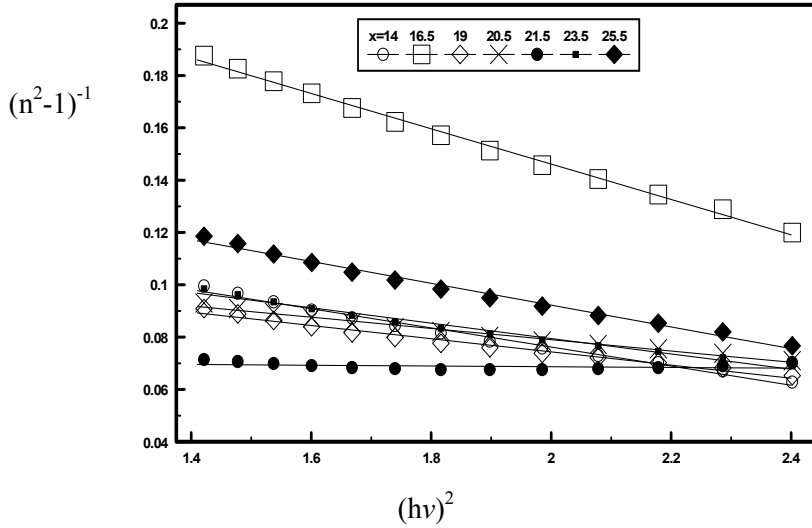


Fig. 9. Variations of  $(n^2-1)^{-1}$  with  $E^2=(h\nu)^2$  for  $In_8Ge_xSe_{92-x}$  thin films.

### Effect of annealing on the optical energy gap

After annealing the thin films of different germanium ratios ( $x = 14, 16.5, 19$  and  $23.5\%$ ) at temperatures ( $T_g + 60K$ ) for different periods of annealing time (5, 10, 20, 30, 40, 50 and 60 mins.), the absorption coefficient  $\alpha$  and then the energy gaps  $E_g$  have been calculated and recorded in table 2 using the same steps explained previously.

Table 2 Variation of  $E_g$  with respect to annealing temperature  $T_a$  and time  $t_a$ .

$t_a$ (mins)	$T_a = 539K$ $x = 14\%$	$T_a = 518K$ $x = 16.5\%$	$T_a = 535K$ $x = 19\%$	$T_a = 578K$ $x = 23.5\%$
	$E_g$ (eV)	$E_g$ (eV)	$E_g$ (eV)	$E_g$ (eV)
0	1.710	1.740	1.790	1.760
5	1.750	1.750	1.845	2.000
10	1.715	1.745	1.879	1.990
20	1.660	1.755	1.846	1.980
30	1.630	1.705	1.847	1.970
40	1.700	1.725	1.845	1.960
50	1.580	1.765	1.847	1.950
60	1.575	1.655	1.848	1.940

It is noticed from table 2 that the values of  $E_g$  increased due to annealing for 5 minutes for the five compositions. The film of  $x = 23.5\%$  showed continuous decrease of  $E_g$  with more prolongation of time of annealing after 5 minutes. This film of  $x = 19\%$  seem to be unaffected by annealing time after 20 minutes of annealing. The two compositions of  $x = 15$  and  $16.5\%$  did not show sequence change with increasing annealing time. The observed variations of  $E_g$  with  $t_a$  for

these annealed thin films can be interpreted in the basis of the effects of two oppositely affecting reasons of the annealing process; a- The increase of  $E_g$  with annealing could be attributed to the homogeneity of the network associating with a decrease of the number of defects, thereby the localized states in the band gap decreases [25]. b- The formation of  $\text{In}_2\text{Se}_3$  and  $\text{GeSe}_2$  structural units with In-Se and Ge-Se bonds which have lower bond energies ( equal to 2.09 and 2.12 eV respectively ) compared with the overall mean bond energy of the investigated thin films [26] which leads to the decrease of  $E_g$ .

#### 4. Conclusions

From the optical measurements on the considered  $\text{In}_8\text{Ge}_x\text{Se}_{92-x}$  thin films, it was found that the electronic energy gap  $E_g$  increases with increasing Ge content. Also, there is an abrupt change of  $E_g$  at  $Z \geq 2.65$ . Moreover, the variation of both  $N / M^*$  and  $\epsilon_\infty$  with the coordination number  $Z$  shows an abrupt change at  $Z \approx 2.65$ .

The change of the optical relaxation time  $\tau$  with  $Z$  showed a minimum at  $Z = 2.65$ .

The effect of annealing on the energy gap  $E_g$  is obvious during the first 5 minutes when  $E_g$  increases

#### References

- [1] E. A. Davis, Electronic and Structural properties of Amorphous Semiconductors, Ed. P. G. Lecomber and Mort ( Academic, London and New York) 425 (1973).
- [2] Mott N. F. and Davis E. A., Electronic processes in Non - crystalline Materials (Clarendon Press, Oxford, 1979).
- [3] Andriesh A. M. J. Non-Cryst. Solids **77&78**, 1219 (1985).
- [4] Cimple Z., Kosek F., J. Non-Cryst. Solids **90**, 577 (1987).
- [5] P. Klocek and Kale B. M., SPIE Proc. **344**, 98 (1982).
- [6] Kana,ori T., Terunuma Y., Takahushi S. and Miyashita T., J. Lightwave Technol. **LT-2**, 607 (1984).
- [7] Davis E. A., in " Electronic and structural properties of amorphous semiconductors", edited by P. G. Lecombe and J. Mart ( Academic press, London, New York, 1973) p.425.
- [8] Susuki M, Ohdaira H, Matsumi T, Kumeda M and Shimizn T, Jpn. J. Appl. Phys. **16**, 221 (1977).
- [9] Flamk A. M., Bazin D, Dexpert H., Lagarde P., Hervo C., and Barraud J. Y., *ibid.* **91**, 306 (1987).
- [10] Tohge N., Minami T., Yamamoto Y. and Tamaka M., J. Appl. Phys. **51**, 1048 (1980).
- [11] Abd El Ghanny H. A., Wakkad M. M, Abo Sehli A. and Assraan N., Physica B **371**, 35 (2006).
- [12] Vleck M., Tichy L., Klikorka J. and Triska L., J. Mater. Sci. Lett. **7**, 335 (1988).
- [13] Abd El Ghani H. A., Abd El Rahim M. M., Wakkad M. M., Abo Sehli A., Assran N., Physica B **381**, 156 (2006).
- [14] Vermaak J. S. and Petruzzello J., J. Appl. Phys. **53**, 6809 (1982).
- [15] Yashinkova L. N. and Novoseov S. K., Inorg. Mater. **13**, 1259 (1977).
- [16] Hafiz M. M., Ammar A. A., Al Adl A. I., and Mohamed A., Phys. Status Solidi **76**, 319 (1983).
- [17] Abou El Ela E. H., El Mously M. K., Abdu K. S., J. Mater. Sci. **15**, 871 (1980).
- [18] Mott N. F., Davis E. A. and Stress R., Phil. Mag., **32**, 961 (1975).
- [19] Handerson D. W., J. Non-Cryst. Solids, **30**, 301 (1979).
- [20] Yinnon H. and Uhlmann D. R., J. Non-Cryst. Solids, **54**, 253 (1983).
- [21] Tauc J., 1974, Amorphous and Liquid Semiconductors (Plenum press, New York)
- [22] Theye M. L., 1974, Proceeding Fifth International Conference on Amorphous and Liquid Semiconductors Vol. 1, Garmisch- Partenkirchen, 1973, Taylor and Francis, London)P.479.

- [23] Bube R. H., 1974, *Electronic Properties of Crystalline Solids* (Academic Press, New York).
- [24] Lostak P., Novotny R., Urbanova E. and Horak J., *Phys. Stat. Solidi* **113**, 615 (1989).
- [25] Chaudhuri S., Biswas S. K. and Choudhury A., *J. Mater.Sci.* **231**, 4470 (1988).
- [26] Tichy L. and Ticha H., *J. Non-Cryst. Solids* **189**, 141 (1995).
- [27] Turnbull D. and Cohen M. H., (*Modern Aspects of the Vitreous State*), edited by J. D. Mackenzie ( Butterworth, London, 1960) pp.38-62